



Microseismicity analysis in the geothermal area of Torre Alfina, Central Italy

Arianna Lisi · Alessandro Marchetti · Alberto Frepoli · Nicola Mauro Pagliuca · Giuliana Mele · Maria Luisa Carapezza · Marco Caciagli · Daniela Famiani · Alessandro Gattuso · Thomas Braun

Received: 1 February 2019 / Accepted: 13 August 2019 / Published online: 11 October 2019
© Springer Nature B.V. 2019

Abstract The geothermal field of Torre Alfina is located in central Italy at the northern edge of the Vulsini Volcanic District, the northernmost area of the so-called Quaternary Roman Co-Magmatic Province. In the framework of a medium-enthalpy geothermal exploitation project, INGV installed a local seismic network close to the future geothermal production site for monitoring natural local seismicity. In this paper, we show the results of a study of the microseismicity recorded from June 2014 to May 2016 in a small area of about 10 km² around Torre Alfina. Analyzing seismic signals recorded by a local temporary network of ten short-period stations and by four permanent stations of the INGV national seismic network, we detected 846 local earthquakes. Then, we accurately relocated

799 events using HypoDD code. Our results show that the region of Torre Alfina is characterized by intense microseismicity, with hypocentral depths between 3 and 7 km and with moderate magnitudes between $M_d = 0.1$ and $M_L = 2.8$. Moreover, more than half of the earthquakes are grouped into six main swarm-like clusters each lasting few days. Furthermore, we computed 36 well-constrained fault plane solutions, which show a clear transtensional deformation regime in the whole study area. Three main tectonic directions have been evidenced from the focal mechanisms analysis: E-W, WSW-ENE, and NW-SE. The understanding of the seismogenic structural setting of the Torre Alfina geothermal field, and the study of its background natural seismicity can be of great importance in recognizing any possible future seismicity induced by the exploitation of the field.

A. Lisi (✉) · N. M. Pagliuca · G. Mele · M. L. Carapezza · D. Famiani · A. Gattuso
Istituto Nazionale di Geofisica e Vulcanologia, Sezione di Roma 1, Italy
e-mail: arianna.lisi@ingv.it

A. Marchetti · A. Frepoli
Istituto Nazionale di Geofisica e Vulcanologia, Centro Nazionale Terremoti, Rome, Italy

M. Caciagli
Istituto Nazionale di Geofisica e Vulcanologia, Sezione di Bologna, Italy

A. Gattuso
Istituto Nazionale di Geofisica e Vulcanologia, Sezione di Palermo, Italy

T. Braun
Istituto Nazionale di Geofisica e Vulcanologia, Sezione di Roma 1, Osservatorio di Arezzo, Italy

Keywords Geothermal field · Earthquake location · Microseismicity · Focal mechanism · Central Italy

1 Introduction

Most of the earthquakes in central Italy occur in the axial and external zones of the Apennines, with magnitudes up to 6.8 and hypocentral depths within the upper 10–15 km (Console et al. 1993; De Luca et al. 1999; Galadini and Galli 2000; Alessandrini et al. 2001; Chiarabba et al. 2005; Pace et al. 2006; Faenza and Pierdominici 2007; ISIDE working group 2016). Seismicity is directly connected to the post-orogenic tectonic evolution of the Apennines (e.g., Brozzetti and Lavecchia 1994; Frepoli and Amato

1997; Collettini et al. 2000; Di Bucci and Mazzoli 2002; Boncio et al. 2004).

The internal (western) part of the Apennines is characterized by crustal thinning, widespread Quaternary volcanism (e.g., Malinverno and Ryan 1986; Jolivet et al. 1998; Peccerillo 2005; Peccerillo and Martinotti 2006; Avanzinelli et al. 2009), and weak seismicity with low-to-moderate magnitude occurring in the upper crust at depths of 3 to 10 km (e.g., Selvaggi and Amato 1992; Cameli et al. 1993; Batini et al. 1995; Di Bucci and Mazzoli 2002). Earthquakes occurring in the geothermal areas of Larderello-Travale and Mt. Amiata (Tuscany region), and Latera and Bolsena (northern Latium region), are likely related to active faults generated by confining pressurized hydrothermal fluids (Buonasorte et al. 1987; Cameli et al. 1993; Liotta and Ranalli 1999; Bellani et al. 2004; Braun et al. 2017, 2018).

Recently, a private industrial company, ITW&LKW Geotermia Italia SpA (ITW&LKW hereinafter), requested a license for the production of geothermal electric energy from the medium-enthalpy geothermal field of Torre Alfina, located north of the Bolsena Lake (Fig. 1). The project conceived the development of two pilot plants of 5 MWe each, with no gas emission in the atmosphere and total re-injection of the extracted fluids into the provenance reservoir. In 2013, in the framework of a research contract between National Institute of Geophysics and Volcanology (INGV) and ITW&LKW, INGV was commissioned to install a multi-parameter system for the monitoring of soil CO₂ gas emission, seismicity, and subsidence in the area where it was planned to drill the producing and reinjecting geothermal wells.

In particular, based on the guidelines for geothermal energy exploitation as established by the Italian Ministry of Industry and Economic Development (MISE) in 2014 (called ILG-2014, hereafter, Dialuce et al. 2014), industrial companies are requested to record the natural seismicity in the future production area, for at least 12 months before the beginning of the exploitation.

In this paper, we present the results of a study of the microseismicity recorded from June 2014 to May 2016 in the area of Torre Alfina. We analyzed velocimetric seismic data recorded by the local temporary network called ReMoTA consisting of ten stations installed by INGV between June 2014 and December 2015 (Fig. 1) and by four permanent stations (SACS, LATE, MGAB, and MCIV) of the INGV national seismic network (INGV-RSN hereafter). ReMoTa seismic stations are equipped with a three-component short-period

seismometer, except station TA06 where a broad band seismic sensor is installed; the four INGV-RSN permanent stations are equipped with a very broad band sensor, and in three of them, also an accelerometric sensor is installed.

In the present contribution, we accurately locate more than 800 local recorded earthquakes and compute 36 fault plane solutions to characterize the temporal and spatial evolution of the local seismicity and to define the active tectonic structures. The understanding of the seismogenic structural setting of the Torre Alfina geothermal field and the study of its background natural seismicity will be of fundamental importance in recognizing any possible future seismicity induced by the exploitation of the field.

2 Geologic setting of the Torre Alfina geothermal field

The geothermal field of Torre Alfina is located at the northern edge of the Vulsini Volcanic District (VVD) (e.g., Sparks 1975). It is bounded by the Meso-Cenozoic ridge of Mt. Cetona to the north, the Bolsena lake caldera to the south, the Radicofani basin to the west, and the Tevere-Paglia basin to the east (Passerini 1964; Nappi et al. 1995) (Fig. 2). Between Torre Alfina and the Bolsena Lake, the Radicofani and Tevere-Paglia graben join into a single basin (Buonasorte et al. 1987).

The VVD is the northernmost extension of the so-called Quaternary Roman Co-Magmatic Province (Washington 1906) whose volcanic products encompass the entire spectrum of potassic and ultra-potassic rock types (Sparks 1975; Barberi et al. 1994; Palladino and Simei 2005a, b).

The Vulsini activity lasted from 0.6 to 0.1 Ma and occurred from several craters (Varekamp 1980) with two main centers: the first one coincides with the present Bolsena Lake, a volcano-tectonic depression developed after large pyroclastic eruptions (Nicoletti et al. 1981; Trigila 1985); the second and more recent one is the Latera volcanic complex, west of the Bolsena lake, whose caldera collapsed after large pyroclastic eruptions about 0.28 Ma (Nappi et al. 1991).

In the southern Tuscany, beneath the surficial volcanic cover, a Miocene-to-Quaternary post-orogenic sedimentary sequences (Neoautochthonous complex) (Martini and Sagri 1993; Liotta, 1994; Pascucci et al. 2006; Brogi and Liotta 2008; Brogi 2011; Brogi et al.

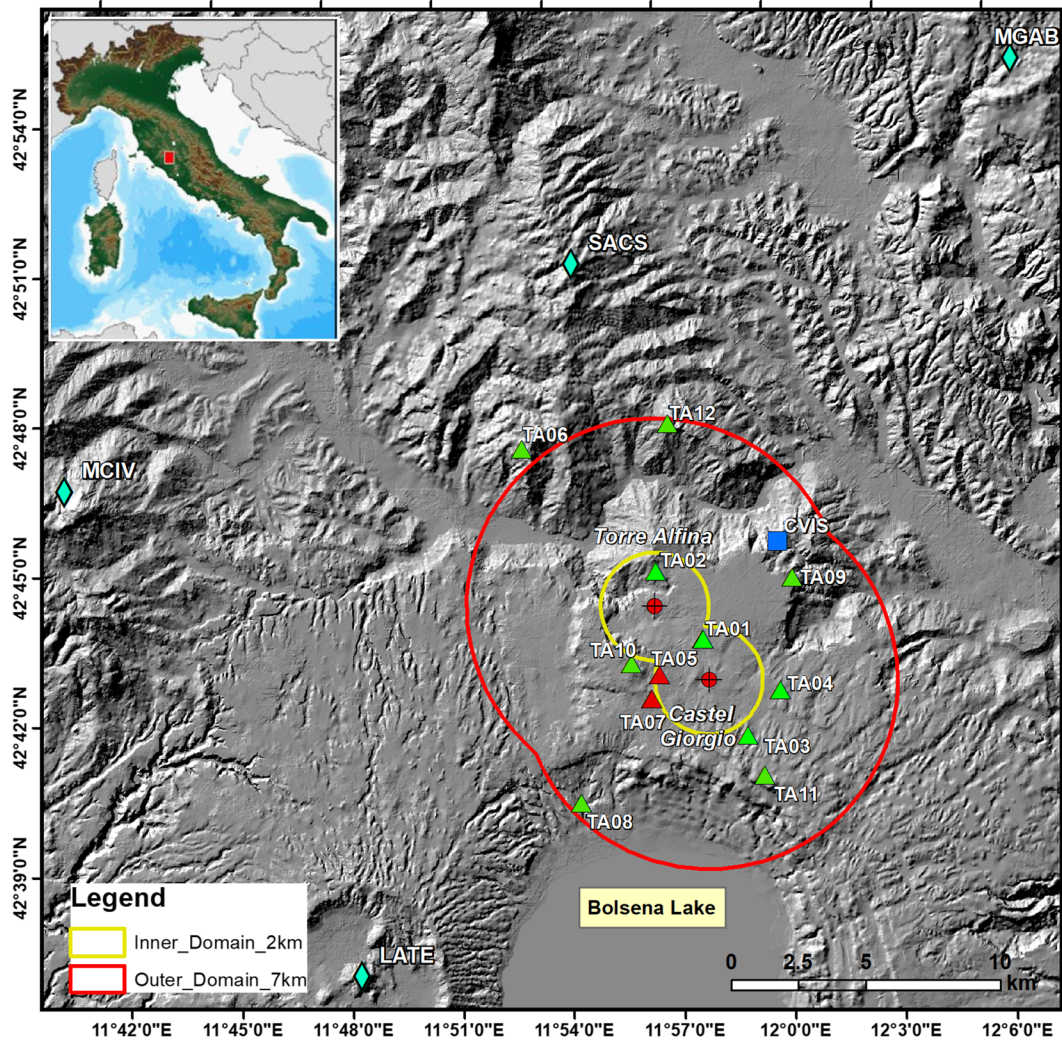


Fig. 1 Area of Torre Alfina/Castel Giorgio (Study area), showing the location of the ten seismic stations of the temporary local ReMoTA network (green triangles). Red triangles indicate sites where stations were installed only for a short time due to high level of anthropic noise. Red dots depict the planned geothermal re-injection sites. Yellow and red curves confine the inner/outer

domain, with a radius of 2 km and 7 km, respectively, around the production/re-injection wells (Terlizzese 2016). The station CVIS belongs to the Regional Accelerometric Network (RAN) of the Umbria region. Light blue diamonds indicate the four permanent stations of the INGV-RSN used in this work. The black rectangle includes the area enlarged in Figs. 5 and 11

2013, 2014) unconformably overlie the oceanic-derived units of the Ligurian domain, consisting of remnants of Jurassic oceanic crust, its Jurassic-Cretaceous mainly clayey cover, and Cretaceous-Oligocene turbidites, which in turn covers continental-derived units of the Tuscan domain (Meso-Cenozoic carbonatic and terrigenous sequences of the Tuscan nappe) (Fig. 2). The upper portion of the Tuscan formation is characterized mainly by marly limestone and shales and is referred to as the “Scaglia formation.” The underlying regional basement is made of Triassic and Paleozoic

metamorphic rocks (Barberi et al. 1994; Brogi and Liotta 2008). Below the Tuscan nappe, the Umbria-Marchigian Unit was encountered at depth by deep boreholes south-east of the M. Cetona (e.g., Torre Alfina 15 in Figs. 3 and 4). The units of Tuscan nappe are exposed in NNW-SSE-trending (as in the Mount Cetona area) and N-S-trending (as in the Mount Labbro area) elongate structural highs bounded by extensional and transtensional faults (e.g., Bonciani et al. 2005; Brogi and Fabbri 2009; Carmignani et al. 2013) (Figs. 2b and 3).

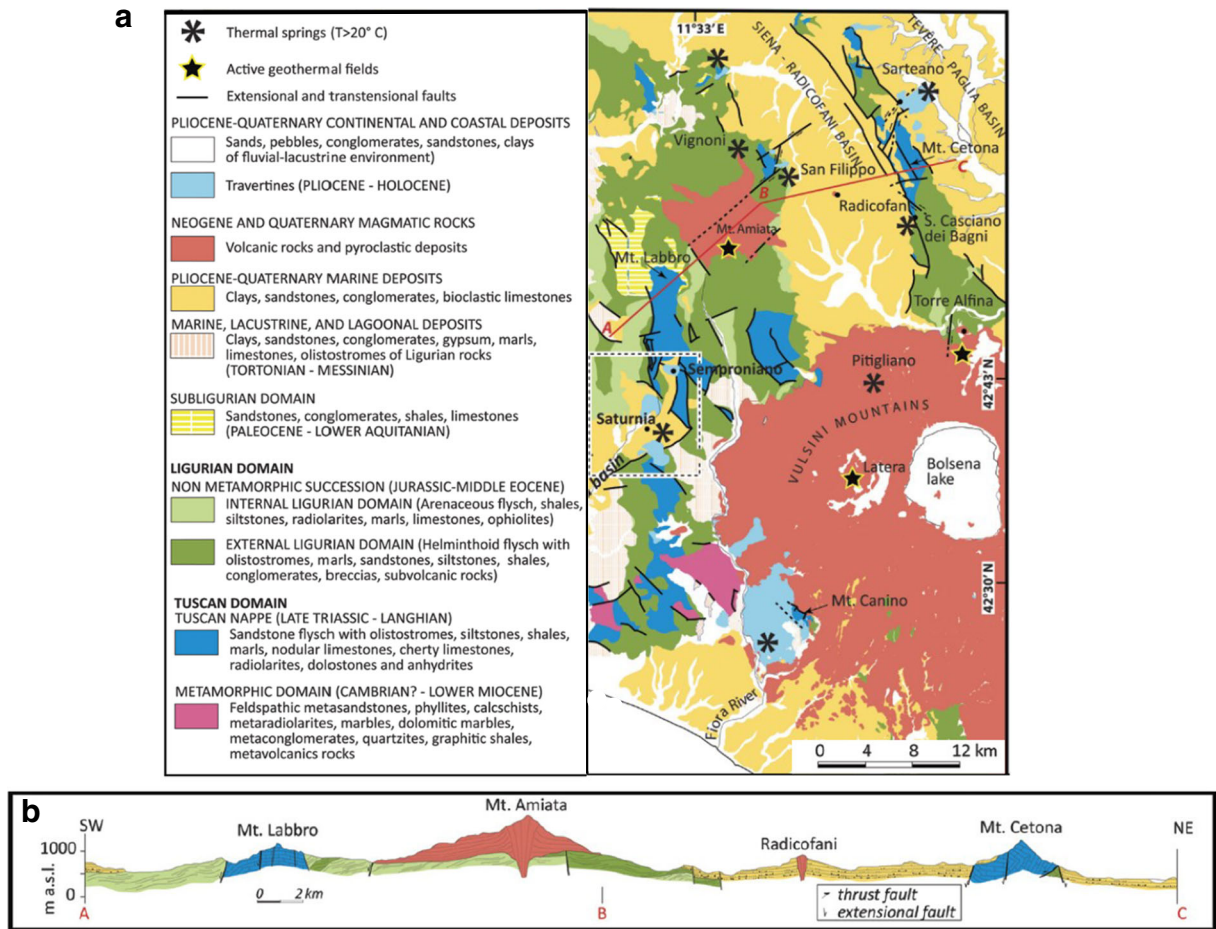


Fig. 2 a Geological-structural map of south-eastern Tuscany (modified after Vignaroli et al. 2016). The black rectangle indicates the study area. **b** Geological cross-section through the Mount

Amiata volcanic district showing post-orogenic structures such as faults, sedimentary basins, and volcanic districts. See the A-B-C cross-section track in **a**

The Early Miocene compressional tectonics produced several NE-oriented thrusts involving the Meso-Cenozoic rocks, detached from the metamorphic basement, and the allochthonous flysch. Since the Langhian-Serravallian (middle Miocene), an extensional process was active generating normal faults and transversal strike-slip structures that dissected the previously formed fold-thrust belt producing *horst-and-graben* structures, generally NNW-SSE oriented (Barchi et al. 1998; Carmignani et al. 1994; Jolivet et al. 1998; Acocella and Funicello 2006; Brogi and Liotta 2008; Brogi et al. 2010). Southern Tuscany is characterized by main NW-SE-trending and minor NE-SW-trending Miocene to Quaternary sedimentary basins formed during the extensional process and bounded by extensional-to-transtensional structures (Martini and Sagri 1993; Liotta 1994; Pascucci et al. 2006; Brogi and Liotta 2008; Brogi 2011; Brogi et al. 2013, 2014). Some of these

include the Tevere-Paglia, Siena-Radicofani, and Albegna basins. The Quaternary volcanism occurred in sites where the NNW-SSE Plio-Pleistocene normal faults were crossed by younger transversal faults with a large component of horizontal displacement (Toro 1978; Acocella and Funicello 2006).

The post-orogenic deposits and the flysch complexes show generally low permeability and constitute the impervious cover of the geothermal field, whereas the geothermal reservoir is represented by the underlying carbonate Mesozoic rocks, usually characterized by secondary permeability due to fracturing. In the Torre Alfina area, the geothermal reservoir is hosted within an uplifted N-S-trending carbonatic anticline structure.

As shown in Fig. 3, below a shallow volcanic cover of VVD deposits, the allochthonous Ligurian units overlie the Tuscan units whose top has been found at a minimum

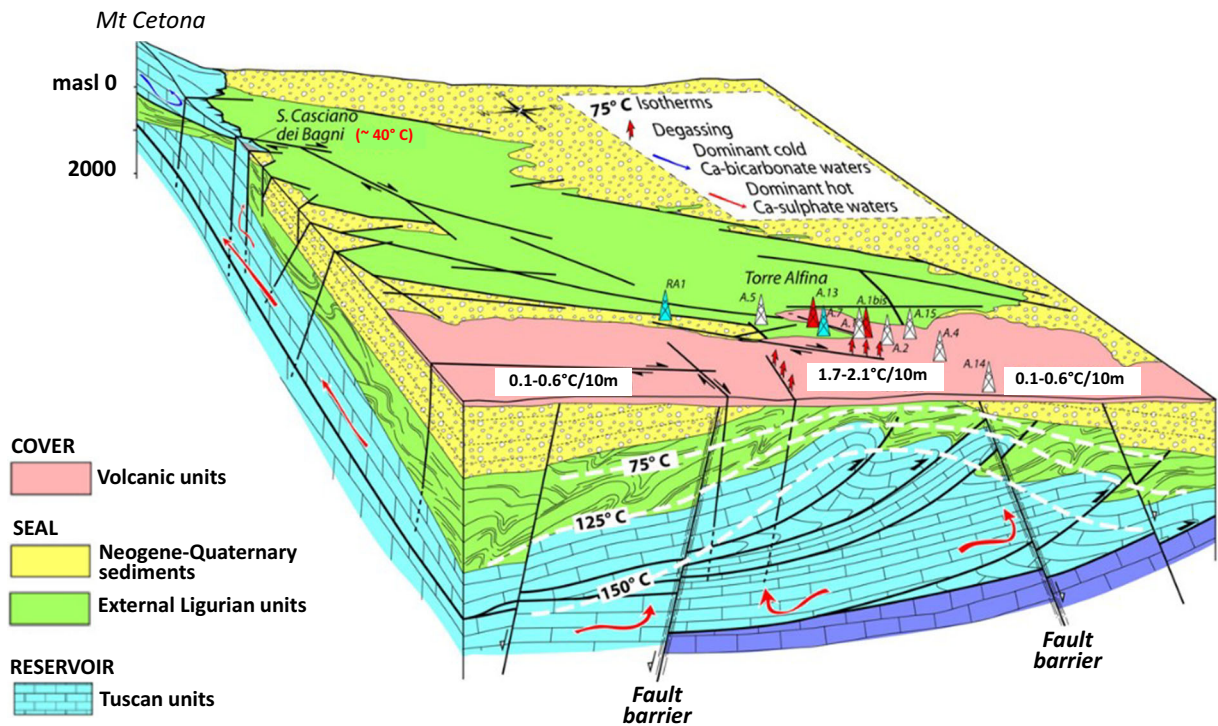


Fig. 3 Block diagram showing the geological and structural setting of the Torre Alfina geothermal field with location of the geothermal wells and isotherms in °C (dashed white lines), after

Vignaroli et al. (2013). The lowermost purple level represents the Umbrian Mesozoic limestones

depth of about 600 m (Buonasorte et al. 1988). The reservoir rocks outcrops north of the geothermal field, in San Casciano dei Bagni village, i.e., at the southern termination of the Mt. Cetona ridge (Fig. 2), which is considered as a possible recharge area of the geothermal system of Torre Alfina (Buonasorte et al. 1988). However, the hydrological connection of Torre Alfina reservoir with Monte Cetona ridge has been questioned for structural reasons by Vignaroli et al. (2013) who suggested that the Torre Alfina recharge may come from Bolsena Lake.

The anomalously high heat flow observed in this area, as well as in all Tuscany and Latium Quaternary volcanic complexes, is related to the long-lived volcanism that has been active for about 1 million years, and due to the cooling of subvolcanic bodies at shallow depth (Barberi et al. 1994; Cameli and Fiordelisi 1988).

The large difference in permeability between the Ligurian flysch and the underlying limestones forms a structural trap that accumulates CO₂ in a pressurized gas cap located at the reservoir top. A set of mainly normal faults, some of them possibly still active, confines the structural high (Fig. 3). A detailed survey of diffuse soil CO₂ flux in the Torre Alfina geothermal area has shown

the presence of a single anomaly at the Solfanare gas manifestation, south of Torre Alfina village, where the composition of the emitted gas is identical to that produced by a geothermal well tapping the reservoir gas cap (Carapezza et al. 2015). Although there is no surface evidence, the authors hypothesize, based on the geometry of the gas flux anomaly, the presence of a NNW-SSE fault connecting the deep geothermal reservoir to the surface.

Geothermal wells, drilled to a maximum depth of 2710 m, proved in the Torre Alfina reservoir the presence of medium-enthalpy hot water with a temperature of 120–140 °C (Buonasorte et al. 1988). A 4826-m deep geothermal well found a thick reservoir made of carbonatic sequences of the Tuscan and Umbrian series, with a temperature range of 140–210 °C (Buonasorte et al. 1991).

Vignaroli et al. (2013) proposed that the geothermal field of Torre Alfina is composed by different compartments, where active tectonic structures play a key role in producing renewed permeability distribution and hydrothermal circulation within the reservoir. Therefore, the microseismicity study of the area could be really helpful to better define the details of its structural setting.

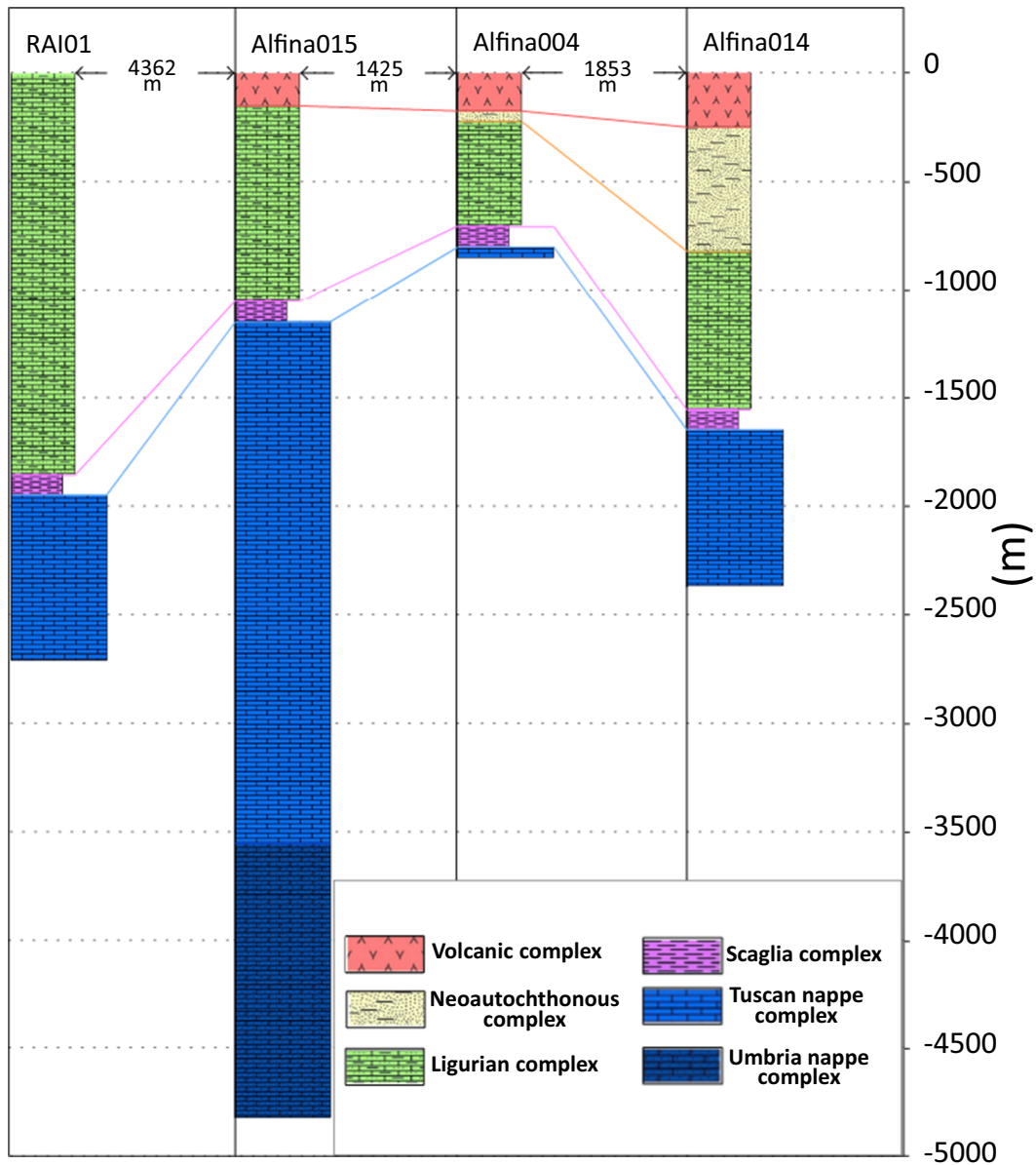


Fig. 4 Stratigraphic columns of four wells drilled in the Torre Alfina geothermal reservoir (modified after Volpi et al. 2018): RAI01, Alfina004, and Alfina014 wells belong to the first drilling

campaign (1971–1972), while the deepest Alfina015 well was drilled on 1987–1988. The well location is shown in Fig. 3 as RA1, A4, A14, and A15 respectively

3 Analysis of the local seismicity

3.1 Historical seismicity

The geothermal area between Mt. Amiata and Bolsena Lake is characterized by moderate seismicity. The Parametric Catalog of Italian Earthquakes (CPTI, Rovida et al. 2016) reports 21 earthquakes since 1000 AD with a maximal intensity I_0 in a range

between VI and IX, based on MCS (Mercalli-Cancani-Sieberg) scale. The strongest events are the equivalent magnitude M_e 5.6 of 1276 A.D. with an epicenter near Orvieto village and the M_e 5.8 of 1695 A.D. with an epicenter east of Bolsena Lake (Guidoboni et al. 2018). The only historical earthquakes that have damaged the small village of Torre Alfina occurred in 1919 near Mt. Amiata (M_e 5.3) and in 1957 near Castel Giorgio (M_e 4.9).

3.2 Instrumental seismicity

The study area (latitude 42.6–42.81 N, longitude 11.8–12.1 E, Fig. 1) is characterized by a shallow seismicity (at depths of 3 to 11 km) with magnitudes generally lower than 3.5. Only a few earthquakes have occurred at depths of 15 to 25 km. The locations and magnitude information were obtained from the ISIDE online catalog <http://iside.rm.ingv.it> (ISIDE working group 2016). The space-time distribution of the seismicity recorded by the INGV-RSN from January 1985 to June 2014, before the period analyzed in this paper, is shown in Fig. 5a, b. The evident increase of number of earthquakes is exclusively due to the extension of the INGV-RSN during the last 10 years that lead to a significant lowering of the detection threshold. It is noteworthy that seismic activity mainly emerges in clusters that have a short duration in time. The cluster of February (7–12) 1992 consists of about 40 events, six of them with $M_L \geq 3$, occurred at shallow depths (3–7 km) near Castel Giorgio, in less than 1 week. On 25 November 2010, 26 events have been recorded some kilometers north of Acquapendente with maximum magnitude $M_L = 2.1$.

Buonasorte et al. (1987) analyzed the seismicity recorded from 1978 to 1986 in the geothermal area near Latera, Bolsena, and Torre Alfina by a local ENEL

network. More than 1000 earthquakes with the maximum magnitude 2.9 were detected by this network. Only 1% of this dataset has magnitudes higher than 2.4. The earthquakes mainly occurred outside the carbonate anticline that host the geothermal field of Torre Alfina area. In particular, Buonasorte et al. (1987) associated the shallower hypocenters to the fault-step caldera of the Bolsena Lake and to the fault zone bounding the eastern flank of the Radicofani basin, between Mt. Cetona and the Acquapendente village.

For this study, we manually picked P- and S-wave arrival times of earthquakes recorded in the period June 2014–May 2016 by the 10 stations of the local network ReMoTA and by the permanent stations SACS, LATE, MGAB, and MCIV (Fig. 1). For the strongest earthquakes, we added the readings of the Italian Seismic Bulletin (hereafter BSI, doi:<https://doi.org/10.13127/BOLLETTINO/2016.03>). Figure 6a and b show two examples of the analyzed seismograms recorded at two different stations, where a swarm-like seismic activity is evidenced.

Events were located using the Hypoellipse code (Lahr 1999) and a velocity model shown in Fig. 7. It is based on the velocity model, used by INGV for seismic monitoring and Italian seismic bulletin, for deeper layers and was merged for the upper 7 km with a model by

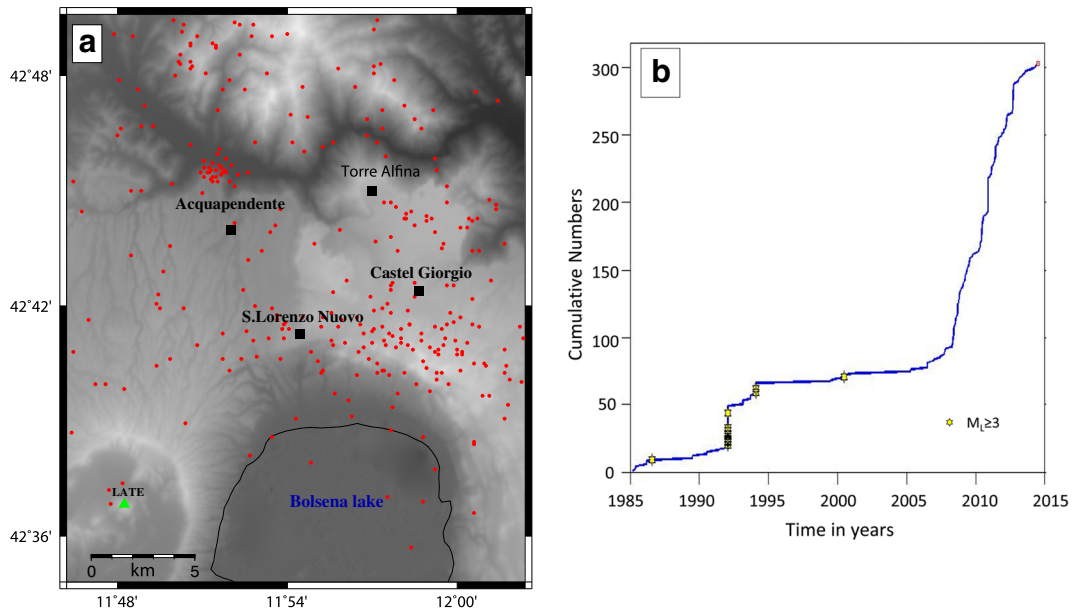


Fig. 5 a Map of 303 epicenters of events recorded by the INGV-RSN from January 1985 to June 2014 in the study area. The green triangle shows the position of the INGV-RSN permanent station, LATE. b Cumulative number of earthquakes occurred from January 1985 to June 2014. Yellow stars indicate earthquakes with $M_L \geq 3$

LATE. b Cumulative number of earthquakes occurred from January 1985 to June 2014. Yellow stars indicate earthquakes with $M_L \geq 3$

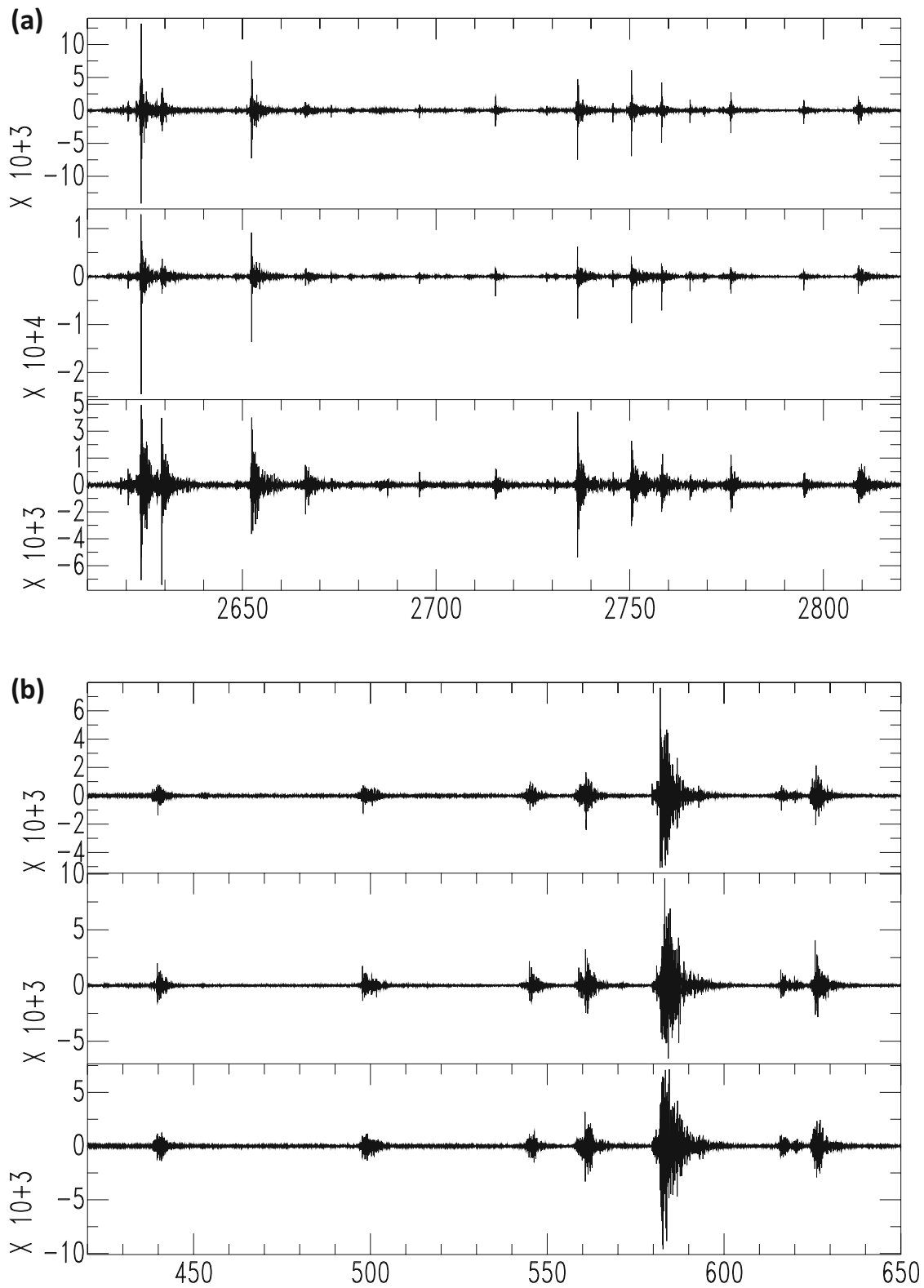


Fig. 6 a, b Examples of three-components short-period seismograms recorded at TA02 and TA05 stations on December 21st and December 24th respectively. The length of the windows is about 4 min

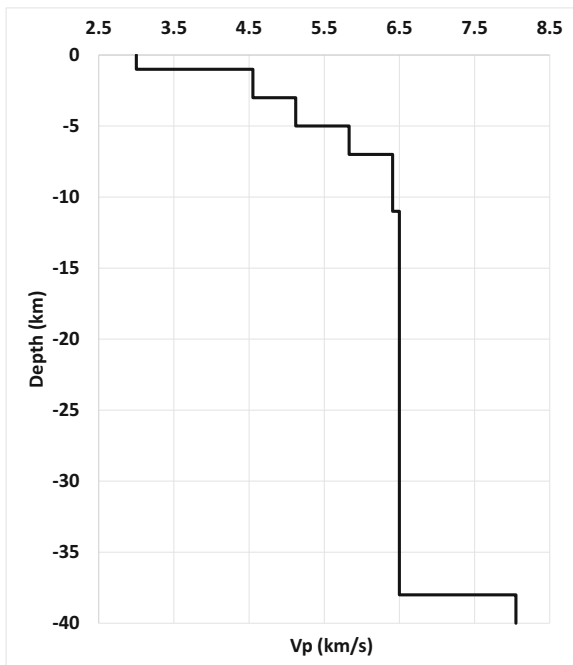


Fig. 7 P-wave velocity model used in this study, obtained by combining the velocity model of Chiarabba et al. (1995) for the first 7-km depth and the one used by INGV for the deeper layers

Chiarabba et al. (1995) who obtained the P-wave velocities from a high-resolution tomography inverting 7535 P- and 563 S-wave arrival times of 676 selected earthquakes occurred in the Torre Alfina area and in the geothermal fields of Latera and Mt. Amiata.

In the study area, we localized 846 earthquakes in a magnitude ranging from $M_d = 0.1$ to $M_L = 2.8$. We assigned to arrival time readings a weight based on the picking accuracy (Table 1). Following the location quality criteria of the Hypoellipse code (Lahr 1999), 98% of our dataset shows quality A and B.

To compute the average local V_p/V_s ratio, we applied the modified Wadati method (Chatelain 1978; Pontoise and Monfret 2004). The linear fit of the time difference between the P and S phases (ΔT_p and ΔT_s) for the available station pairs gives a V_p/V_s ratio of 1.87 within

Table 1 Weights assigned to P and S arrival times based on the picking accuracy

Weight	Picking accuracy (s)
0	$0 < i \leq 0.1$
1	$0.1 < i \leq 0.3$
2	$0.3 < i \leq 0.6$
3	$0.6 < i \leq 1.0$
4	$i > 1.0$

a confidence of 95%, a root-mean square (RMS) error of 0.015, and a linear correlation coefficient of 0.96 (Fig. 8). The high V_p/V_s ratio indicates a highly fractured medium, as expected in a volcanic region.

Then, we re-located the 846 events applying the double-difference (DD) location algorithm HypoDD (Waldhauser and Ellsworth 2000; Waldhauser 2001). At each station, the DD residuals are minimized for pairs of earthquakes by weighted least squares using the conjugate gradients method (LSQR) (Paige and Saunders 1982). The code iteratively adjusts the vector difference between nearby pairs of hypocenters, updating the location and the partial derivatives at each iteration. Starting from 846 events, we obtained 799 relocated events satisfying the HypoDD quality criteria.

Figure 9 shows the horizontal and vertical error distribution, RMS and depth of the 846 earthquakes localized with Hypoellipse (left panels) and of the 799 relocated with HypoDD (right panels). The errors associated with the hypocentral determination and the RMS decrease substantially in the HypoDD locations. Hypocentral depths are more concentrated around the 5 km depth using the HypoDD code (Fig. 7).

The cumulative seismic energy is plotted (Hanks and Kanamori 1979) in Fig. 10, while the released seismic energy for each swarm of earthquakes is reported in Table 2. To calculate the released energy, we converted M_d in M_L using the following relationship from Gasperini (2002):

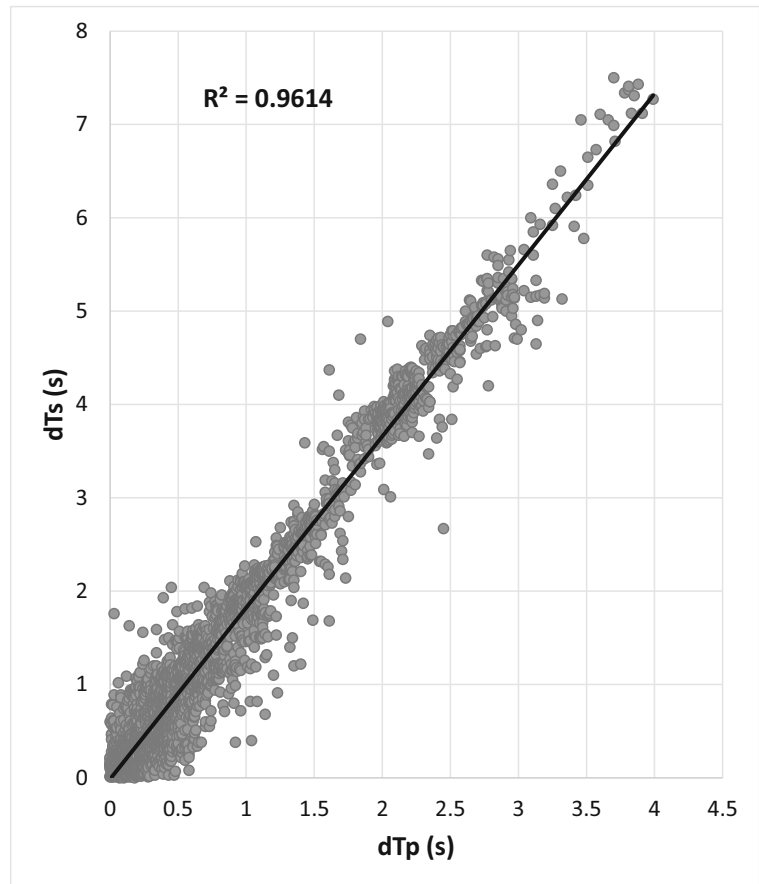
$$M_L = 0.99M_d + 0.05. \tag{1}$$

From Table 2, it is clear that more than half of the earthquakes are grouped into six main clusters and that higher energies are released from the clusters with larger maximum magnitude.

The first significant fast increase in energy in the cumulative curve of Fig. 10 is coincident with the November 2014 cluster and is the largest observed fast increase in energy also if the November 2014 cluster has the lowest number of events (30 earthquakes) and the lowest maximum magnitude ($M_d = 1.7$). The reason for this is that the largest event with $M_L = 2.8$ occurred just 1 week before the November 2014 swarm. Thus, we see in the curve the combined released energy relative to both the cluster and the largest earthquake.

The relocated seismicity is mapped in Fig. 11a while Fig. 11b shows the hypocenters plotted on NE-SW and

Fig. 8 Wadati diagram. Linear fit of ΔT_s versus ΔT_p (S- and P-wave differential time measurements, respectively). The obtained V_p/V_s ratio is 1.868, the root-mean square (rms) error is 0.015, and the linear correlation coefficient (R^2) is 0.96



NW-SE cross-sections, respectively. The seismicity results mainly concentrated in a small region north of Bolsena Lake confined among the villages of Torre Alfina, to the north; S. Lorenzo Nuovo and Acquapendente, to the west; and Castel Giorgio, to the east. Hypocentral depths are ranging from 1 to 9 km. The black and white dots indicated the spread out seismicity while the colored dots are relative to the clustered events. The clustered events occurred in a few days (Table 2) and occurred (each time) in different portions of the study region (Figs. 11 and 12). Figure 12 shows the location in map and in sections of the six main swarms.

Based on the magnitude values and on their spatio-temporal distribution, we consider the clusters as typical swarms; in fact, they are not characterized by the occurrence of a mainshock. In addition, for the analyzed dataset, the largest event we recorded with $M_L = 2.8$ does not belong to any cluster.

The duration magnitude M_d has been calculated through the empirical relationship of the Hypoellipse

code (Lee et al. 1972; Lee and Lahr 1975; Bakun and Lindh 1977):

$$M_d = C_1 + C_2 \log_{10}(D \cdot c) + C_3 E + C_4 Z + C_5 (\log_{10}(D \cdot c))^2, \quad (2)$$

where $C_1 = -0.87$, $C_2 = 2$, $C_3 = 0.0035$, $C_4 = 0$, $C_5 = 0$, D = length of earthquake recording (s), E = epicentral distance (km), Z = hypocentral depth (km), and $c = 1$; therefore, we obtain

$$M_d = -0.87 + 2 \log_{10}(D) + 0.0035E. \quad (3)$$

For the largest events, we reported the values of M_L when available from the BSI (doi:<https://doi.org/10.13127/BOLLETTINO/2016.03>).

Figure 13 shows the coda magnitude distribution of the 846 located earthquakes.

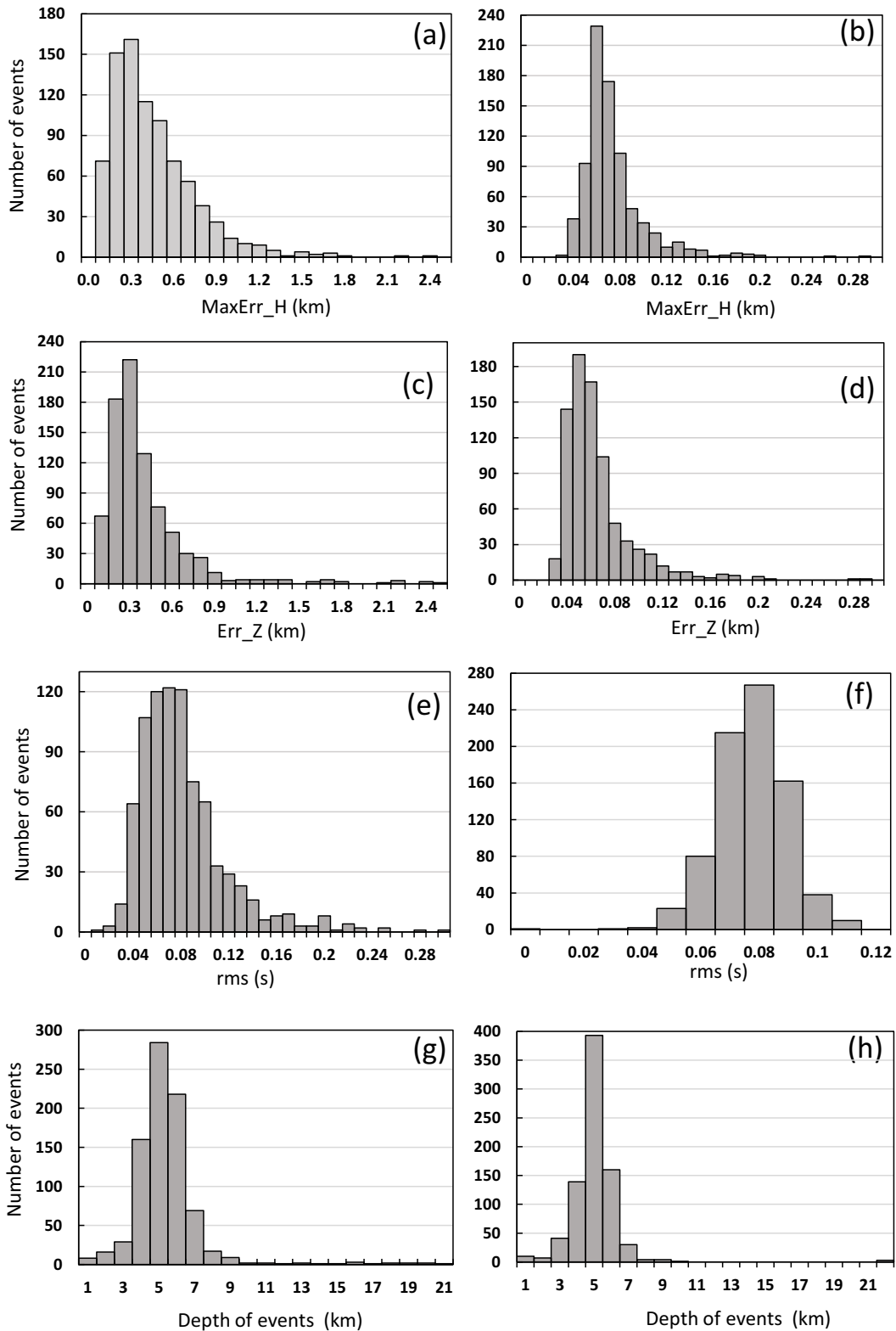


Fig. 9 Comparison between location errors, RMS, and depth distribution obtained for the 846 earthquakes located with Hypoellipse (left panels a, c, e, g) and for the 799 relocated earthquakes with the HypoDD algorithm (right panels b, d, f, h)

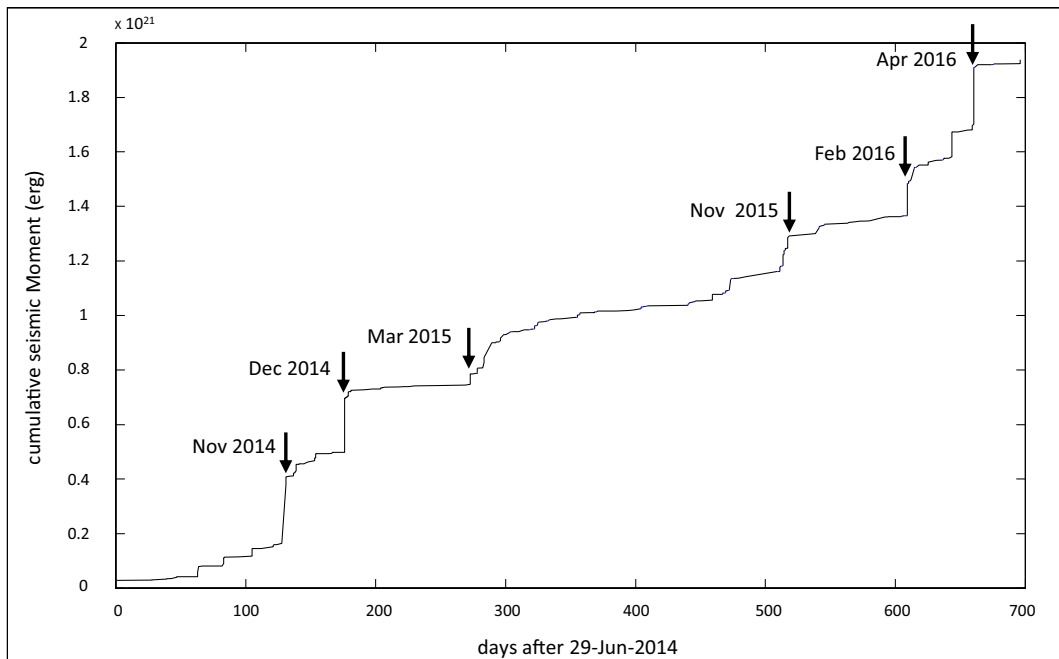


Fig. 10 Cumulative seismic moment of earthquakes relocated with HypoDD. Arrows indicate the six main clusters. The first significant fast increase in energy is due to both the November 2014 cluster and the M_L 2.8 event, which occurred 1 week before the swarm

3.3 Fault plane solutions

We calculated 56 fault plane solutions with at least eight clear first motion polarities using the FPFIT code (Reasenberg and Oppenheimer 1985). Among these, we chose the best 36 solutions with well-distributed polarities on the focal sphere and high-quality factors Q_p and Q_f (outputs of the FPFIT code). The quality factors varies from A to C with decreasing quality.

Q_p gives information about the solution misfit of the polarity data, while Q_f reflects the solution uniqueness in terms of the 90% confidence for strike, dip, and rake. Figure 14 shows the selected focal mechanisms: 12 with

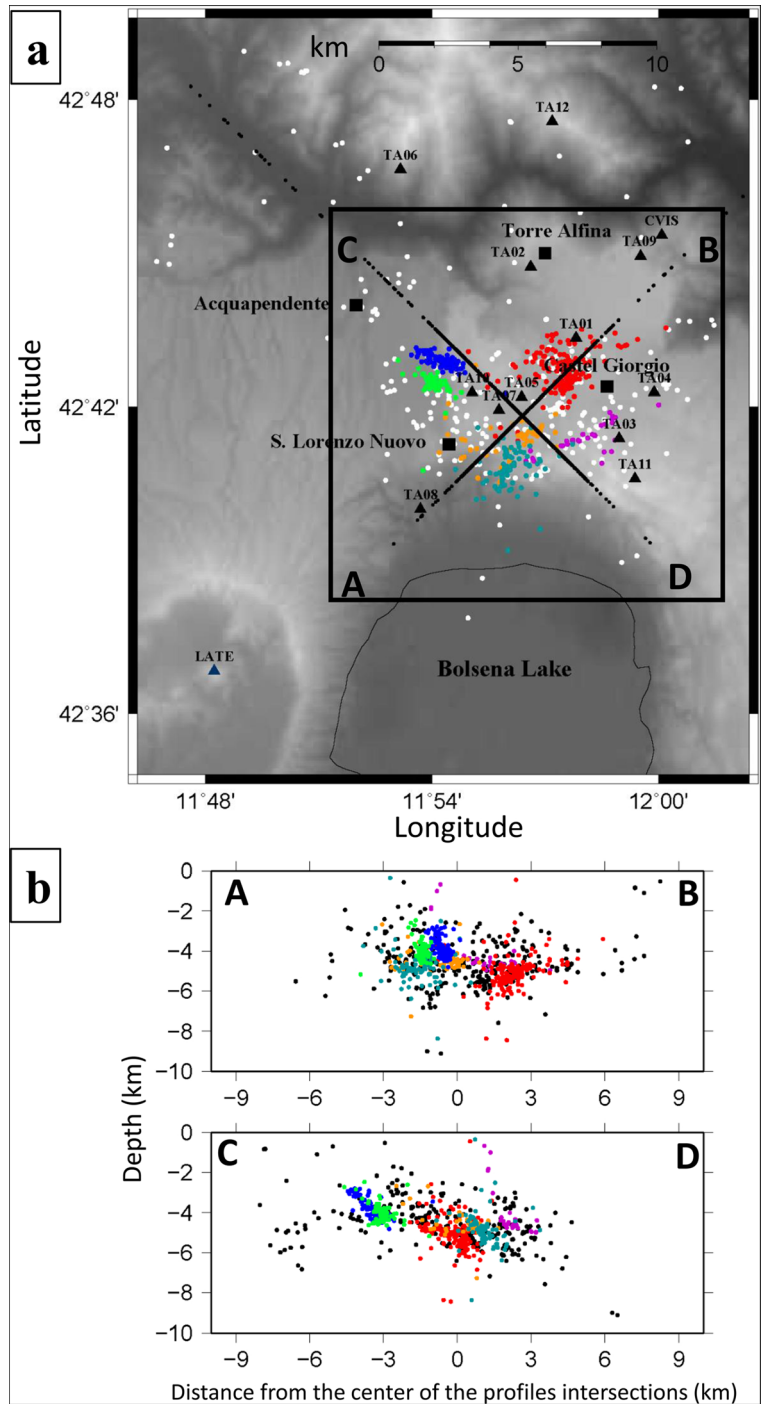
quality AA and 24 with quality AB and BA. The average orientation of the T-axis suggests a NNE-SSW extension regime for the whole study area. Events with selected fault plane solution have magnitude ranging from $M_d = 1.0$ to $M_L = 2.8$ (Fig. 14). There are 17 focal mechanisms with an almost pure strike-slip solution. Most of these solutions belong to the green and blue clusters (Fig. 14). All strike-slip solutions have a small normal component. We do not have enough information to discriminate between the two nodal planes. If the NE-SW nodal plane is the fault plane, then we have a right-lateral motion. There are 13 normal fault solutions with small strike-slip component, while six are pure normal

Table 2 Description of the six main clusters occurred during the study period

No.	Time of occurrence	Number of events ^a	Maximum magnitude	Cumulative seismic moment (erg)
1	2014, November 13–14	30 (purple)	1.7 (M_d)	3.2×10^{19}
2	2014, December 21–26	158 (red)	2.6 (M_L)	2.2×10^{20}
3	2015, March 24–28	53 (orange)	1.7 (M_d)	4.3×10^{19}
4	2015, November 23–29	80 (light blue)	1.9 (M_d)	1.2×10^{20}
5	2016, February 28–March 2	115 (blue)	1.9 (M_d)	1.3×10^{20}
6	2016, April 18–22	76 (green)	2.3 (M_d)	2.4×10^{20}

^a In the second column, the reference color for each cluster is indicated as shown in Figs. 9, 10, and 12.

Fig. 11 **a** Map of the 799 earthquakes relocated with HypoDD. White dots indicate the non-clusterized seismicity; colored dots represent the six clusters: November 2014 (purple), December 2014 (red), March 2015 (orange), November 2015 (light blue), February 2016 (blue), and April 2016 (green). The black rectangle includes the area enlarged in Figs. 10a and 12. **b** In the cross-sections A-B and C-D, black dots indicate the non-clusterized seismicity



(Fig. 14). The largest number of normal fault plane solutions are observed in the red cluster. The event with largest magnitude (M_L 2.8), which does not occur within any cluster, shows a normal fault with a very small strike-slip component. If the fault plane is oriented NW-

SE with dip to the SW, the small strike-slip component has left-lateral motion.

In this study, we considered only double-couple solutions, also if the fluid movement due to the presence of the geothermal field could have an important role in the

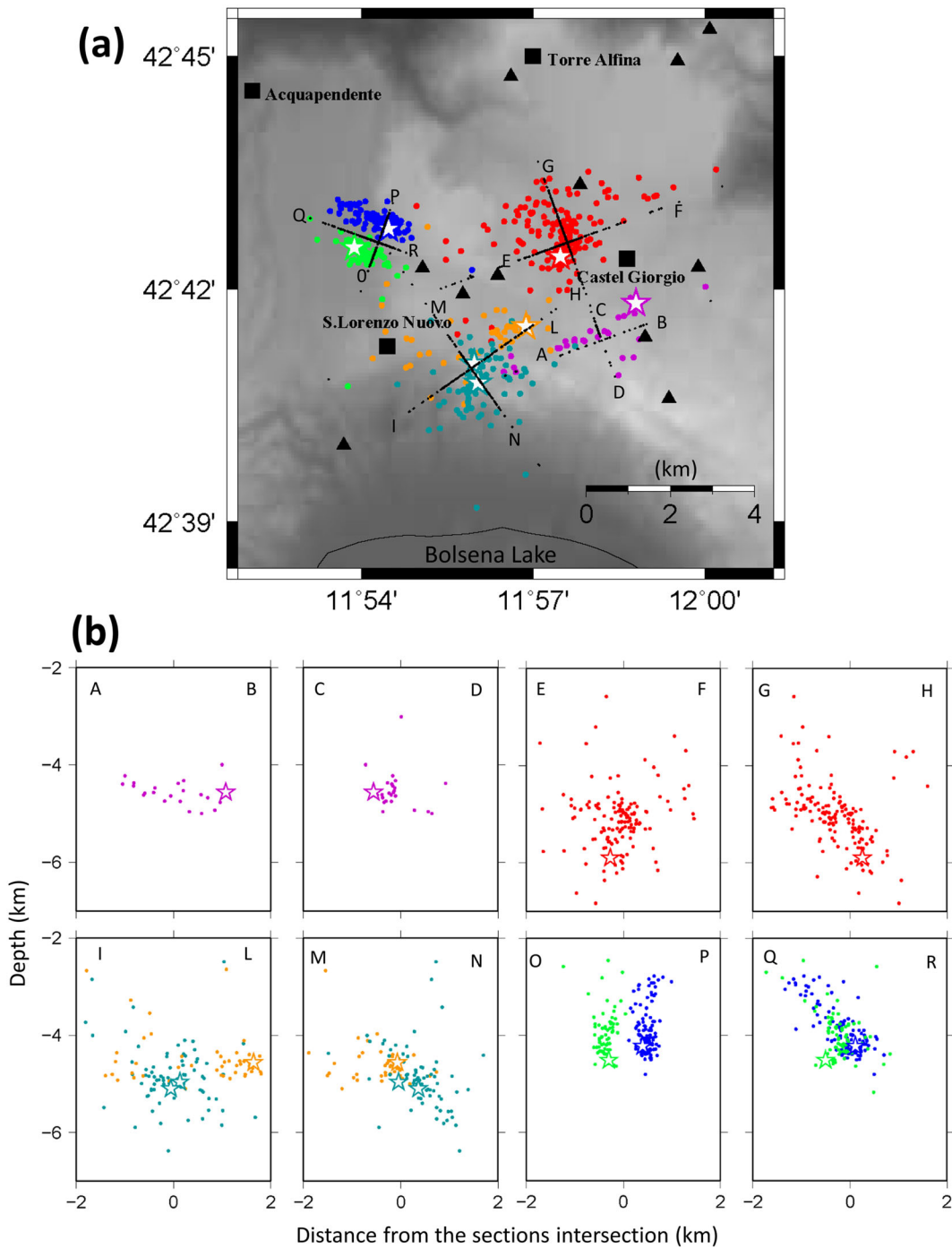


Fig. 12 **a** Map and **b** cross-sections of the six clusters listed in Table 2. The white stars indicate the strongest shock for each cluster

earthquake mechanisms; therefore, we could expect to have for this region some events with non-double-couple mechanisms. We planned to test this possibility using new data recorded after May 2016, when an important seismic

sequence with moderate magnitude events occurred in this area. The new dataset, which we are analyzing, will provide us a higher number of events with enough polarities to calculate also not-double-couple solutions.

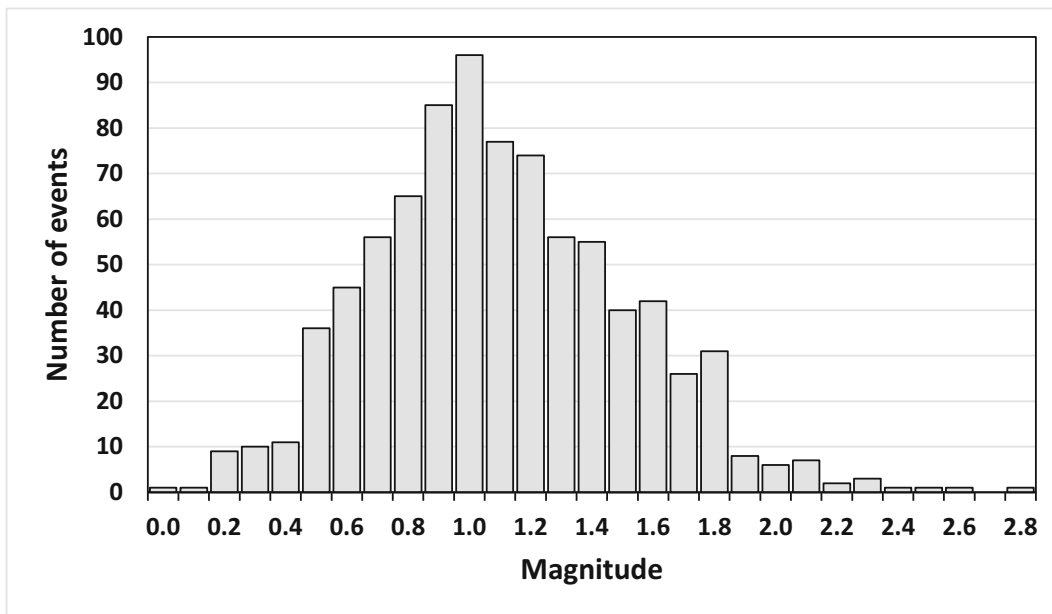


Fig. 13 Distribution of magnitude (M_d) for the 846 located earthquakes

4 Discussion

From June 2014 to May 2016, ten temporary and four permanent stations recorded intense microseismicity occurring in a small area of about 10 km^2 around the geothermal field of Torre Alfina. We accurately located 799 earthquakes with magnitude ranging between $M_d = 0.1$ and $M_L = 2.8$. More than half of the events are grouped into six clusters each lasting for few days; all the clusters are characterized by the absence of a mainshock. This is a typical swarm behavior of volcanic regions.

While the epicenters associated to the 2014 and 2015 clusters do not show a clear alignment, the two clusters occurred in 2016 are both aligned along NW-SE direction (blue and green dots in Fig. 12).

The 2014 and 2015 clusters, located in the eastern and south-eastern part of the study area between the villages of S. Lorenzo Nuovo and Castel Giorgio, occurred in a depth range of 3.5–6.5 km, while the 2016 clusters, located to the north-western edge, are slightly shallower (3–5 km depth). A common feature, at least for the larger cluster in 2014 and for the clusters in 2016, is that the strongest event is deeper (Fig. 12).

The earthquakes located between the Bolsena Lake and Torre Alfina are mainly characterized by normal focal mechanisms while those in the western part are mainly strike-slip. The higher number of seismic

stations in 2016 allowed us to calculate a larger number of focal mechanisms for the two swarms occurred in this year.

All the focal mechanisms show a clear transtensional deformation regime in the area as it has been proposed by Vignaroli et al. (2013). The authors, through a statistical analysis of the collected structural data, grouped the sub-vertical fractures into NNE-SSW and WNW-ESE directions. The WNW-ESE-oriented fractures are consistent with the orientation of the T-axis that we obtained from all the focal solutions.

Three main tectonic directions are clearly evidenced from the focal mechanisms analysis: E-W, WSW-ENE, and NW-SE. This evidence confirms the results obtained by Buonasorte et al. (1987) who, based on a seismicity study of more than 1000 earthquakes, found the same main tectonic directions.

The nine normal fault plane solutions located to the west of Castel Giorgio (four from the December 2014 cluster and five from non-clusterized seismicity), one mechanism north of S. Lorenzo (February 2016 cluster), and one south-east of S. Lorenzo (November 2015 cluster) show a nodal plane E-W oriented with a high southward dip. These solutions are consistent with the existing step faults associated with the caldera depression of Bolsena Lake, also shown by Buonasorte et al. (1987). The authors observed, in the area to the north and east of the

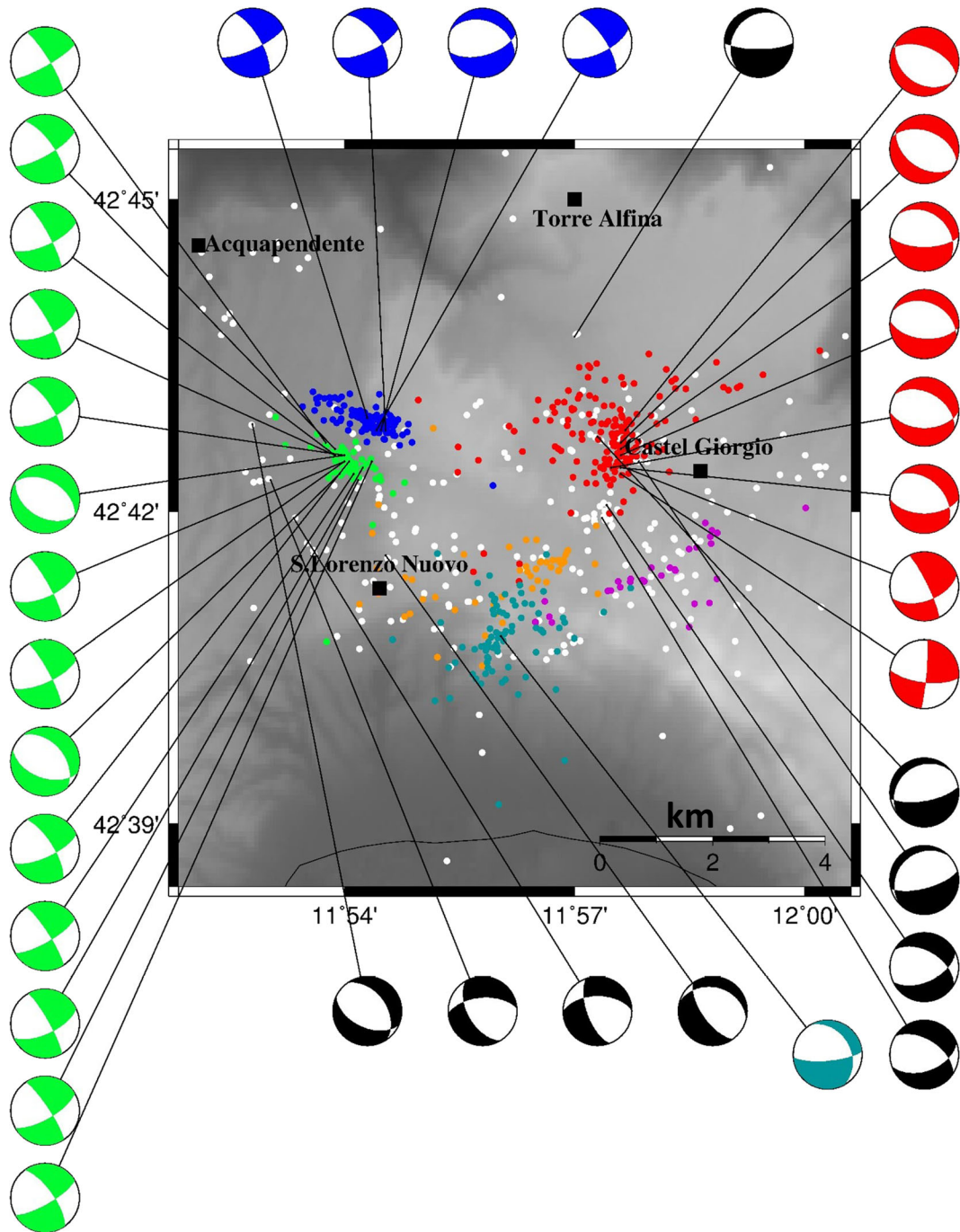


Fig. 14 Map of the epicentral distribution showing also the 36 well-constrained focal mechanisms; ten fault plane solutions from the non-clusterized seismicity, eight from the December 2014

cluster (No. 2 in Table 2), one from November 2015 cluster (No. 4 in Table 2), four from the February 2016 cluster (No. 5 in Table 2), and 14 from the April 2016 cluster (No. 6 in Table 2)

lake, a high density of step faults extending to a distance of at least 7 km from the lake. In the region between S. Lorenzo Nuovo and Bolsena Lake, they computed normal fault plane solutions with nodal

plane striking N80E and dipping 45° southward. Furthermore, step faults were evidenced by a high-resolution seismic reflection survey in the northern part of Bolsena Lake (Buonasorte et al. 1995).

From the analysis of the focal mechanisms associated to the events occurred during the 2016 clusters north of S. Lorenzo Nuovo, we found that 15 of the 18 computed mechanisms indicate a strike-slip solution with a very small normal component. Unfortunately, our data on hypocenter distribution do not provide enough clear information in order to discriminate between the two nodal planes. If we assume the southward high dipping, WSW-ENE-oriented plane as the fault plane, we obtain a dextral transcurrent movement and our fault plane solutions would be very similar to the mechanism calculated by Buonasorte et al. (1987). Furthermore, a structural study on tectonic discontinuities showing evidence of post-orogenic activity in the region between Torre Alfina, Acquapendente, and Castel Giorgio put in evidence a dominant strike-slip motion with dextral kinematics (Vignaroli et al. 2013). In particular, the authors observed in the area around Acquapendente a strike-slip direction WSW-ENE oriented. Alternatively, the fault plane could be the one NNW-SSE oriented, sub-vertical, and with left lateral slip. This kind of kinematics has already been observed further north in the region between Mt. Amiata and Mt. Cetona (Brogi and Fabbrini 2009) but along SW-NE-oriented faults. Quaternary transtensive faults with SW-NE strike generally influence the Pleistocene and present hydrothermal fluids circulation. In the Mt. Amiata region, SW-NE striking Quaternary faults are strictly related to the volcanic activity (Acocella 2000; Acocella and Funicello 2002; Brogi 2008). Focal mechanisms associated with microshocks induced by hydrofractures generally show strike-slip with sub-vertical nodal planes (Raleigh et al. 1976; Carabelli et al. 1984).

The strongest events we recorded with $M_L = 2.8$ and depth of 5 km does not belong to any cluster and occurred at north-west of S. Lorenzo Nuovo village, on the western part of the 2016 clusters. The associated focal mechanism shows normal faulting, but differently from the other normal mechanisms computed in the area, it is consistent with a high-angle west-dipping and NNW-SSE-oriented normal fault with small left-lateral transcurrent. This solution is similar to those found for other two earthquakes, which occurred just north of S. Lorenzo Nuovo, both with $M_d = 1.7$ and with comparable depth. Similar mechanisms have been calculated by Buonasorte et al. (1987) for a small cluster

located at about 4–5 km SW of Acquapendente village. This fault plane solution is consistent with the Early-Middle Pliocene fault system that, exposed for several kilometers in the eastern margin of the Radicofani basin, includes also the main regional fault known as the Cetona Fault (Liotta and Salvatorini 1994; Liotta 1996; Acocella et al. 2002; Brogi and Fabbrini 2009).

The five focal mechanisms with almost pure normal fault plane solutions, consistent with a NW-SE oriented fault plane with a 30° south-west dip, located to the west of Castel Giorgio and to the north of S. Lorenzo Nuovo, may indicate a reactivation of the Miocene south-west-dipping thrust system. Buonasorte et al. (1991) suggested, on the basis of the stratigraphic interpretation of an exploration well in the Torre Alfina area, that the tectonic stacking of the Tuscan and Ligurian units is controlled by a 25° SW dipping NW-SE oriented thrust system.

To consider only double-couple mechanisms could be an oversimplification for this geothermal region, but we are going to calculate also non-double-couple solutions using a more comprehensive dataset including the seismicity recorded in the following years.

5 Conclusions

This study confirms that the region located in the northern edge of the Vulsini Volcanic District is characterized by moderate background microseismicity mainly concentrated within the uppermost 10 km. The computed focal mechanisms are consistent with geological evidence of fault systems in the area. The fault plane solutions highlighted the evidence of a present transtensional deformation regime in a NE-SW direction.

Three different kinematics characterize the active faults in the study area:

- Strike-slip to oblique mechanisms that can be related to the activity of transfer faults
- Normal high-angle plane dipping towards south, which are probably step faults associated to the Bolsena Lake caldera collapse
- NW-SE-oriented normal faults due to the reactivation of the Miocene thrust system.

The lack of seismicity beneath 10 km depth indicate ductile behavior of rocks due to high temperature (up to 400°C) existing at those depths.

Acknowledgments The present study on Torre Alfina geothermal field has been carried out in the framework of a research contract between INGV and ITW & LKW Geotermia Italia spa.

References

- Acocella V (2000) Space accommodation by roof lifting during pluton emplacement at Amiata (Italy). *Terra Nova* 12:149–155
- Acocella V, Funicello R (2002) Transverse structures and volcanic activity along the Tyrrhenian margin of Central Italy. *Boll Soc Geol Ital Spec* 1:739–747
- Acocella V, Funicello R (2006) Transverse systems along the extensional Tyrrhenian margin of Central Italy and their influence on volcanism. *Tectonics* 25:TC2003. <https://doi.org/10.1029/2005TC001845>
- Acocella V, Pascucci V, Dominici G (2002) Basin deformation due to laccolith emplacement at Radicofani (southern Tuscany, Italy). *Boll Soc Geol Ital* 1:749–756
- Alessandrini B, Filippi L, Borgia A (2001) Upper-crust tomographic structure of the Central Apennines, Italy, from local earthquakes. *Tectonophysics* 339:479–494
- Avanzinelli R, Lustrino M, Mattei M, Melluso L, Conticelli S (2009) Potassic and ultrapotassic magmatism in the circum-Tyrrhenian region: significance of carbonated pelitic vs. pelitic sediment recycling at destructive plate margins. *Lithos* 113:213–227
- Bakun WH, Lindh A (1977) Local magnitudes, seismic moments, and coda durations for earthquakes near Oroville, California. *Bull Seism Soc Am* 63:615–629
- Barberi F, Buonasorte G, Cioni R, Fiordelisi A, Foresi L, Iaccarino S, Laurenzi M, Sbrana A, Vernia L, Villa IM (1994) Plio-Pleistocene geological evolution of the geothermal area of Tuscany and Latium. *Mem Soc Geol Ital* 49:63–109
- Barchi MR, De Feyter A, Magnani MB, Minelli G, Piali G, Sotera M (1998) Extensional tectonics in the northern Apennines (Italy); evidence from the CROP 03 deep seismic reflection line. *Mem Soc Geol Ital* 52:527–538
- Batini F, Fiordelisi A, Graziano F, Nafi Toksöz M (1995) Earthquakes and tomography in the Larderello geothermal area: geothermal anomalies and structural features of southern Tuscany. *World Geothermal Congress Proceedings, Florence*, pp 817–820
- Bonciani F, Callegari I, Conti P, Cornamusini G, Carmignani L. (2005) Neogene post-collisional evolution of the internal Northern Apennines: insights from the upper Fiora and Albegna valleys (Mt. Amiata geothermal area, southern Tuscany) *Boll. Soc. Geol. It., Volume Speciale n. 3*, 103–118
- Bellani S, Brogi A, Lazzarotto A, Liotta D, Ranalli G (2004) Heat flow, deep temperatures and extensional structures in the Larderello geothermal field (Italy): constraints on geothermal fluid flow. *J Volcanol Geotherm Res* 132:15–29
- Boncio P, Lavecchia G, Pace B (2004) Defining a model of 3D seismogenic sources for seismic Hazard assessment applications; the case of Central Apennines (Italy). *J Seismol* 8:407–425
- Braun T, Pagliuca NM, Gattuso A, Mele G, Caciagli M, Famiani D, Marchetti A, Badiali L, Frepoli A, Lisi A, Carapezza ML (2017) Installazione della rete di monitoraggio sismico ReMoTA nell'area geotermica di Torre Alfina-Castel Giorgio (Lazio settentrionale-Umbria). *Rapp Tec INGV* 370:1–44 (in Italian)
- Braun T, Caciagli M, Carapezza ML, Famiani D, Gattuso A, Lisi A, Marchetti A, Mele G, Pagliuca NM, Ranaldi M, Sortino F, Tarchini L, Kriegerowski M, Cesca S (2018) The seismic sequence of 30th May - 9th June 2016 in the geothermal site of Torre Alfina (Central Italy) and related variations in soil gas emissions. *J Volcanol Geotherm Res* 359:21–36
- Brogi A (2008) The Triassic and Palaeozoic successions drilled in the Bagnore geothermal field and Poggio Nibbio area (Monte Amiata, Northern Apennines, Italy). *Boll Soc Geol Ital* 3: 599–613
- Brogi A (2011) Bowl-shaped basin related to low-angle detachment during continental extension; the case of the controversial Neogene Siena Basin (Central Italy, Northern Apennines). *Tectonophysics* 499:54–76
- Brogi A, Fabbrini L (2009) Extensional and strike-slip tectonics across the Monte Amiata–Monte Cetona transect (Northern Apennines, Italy) and seismotectonic implications. *Tectonophysics* 476:195–209
- Brogi A, Liotta D (2008) Highly extended terrains, lateral segmentation of the substratum, and basin development: the middle-late Miocene Radicondoli Basin (inner northern Apennines, Italy). *Tectonics* 27:TC5002. <https://doi.org/10.1029/2007TC002188>
- Brogi A, Liotta D, Meccheri M, Fabbrini L (2010) Transtensional shear zones controlling volcanic eruptions: the middle Pleistocene Mt Amiata volcano (inner Northern Apennines, Italy). *Terra Nova* 22:137–146
- Brogi A, Fiolini F, Liotta D (2013) Tectonic and sedimentary evolution of the upper Valdarno Basin: new insights from the lacustrine S. Barbara Basin. *Ital J Geosci* 132(1):81–97
- Brogi A, Capezzuoli E, Martini I, Picozzi M, Sandrelli F (2014) Late Quaternary tectonics in the inner northern Apennines (Siena Basin, southern Tuscany, Italy) and their seismotectonic implications. *J Geodyn* 76:25–45
- Brozzetti F, Lavecchia G (1994) Seismicity and related extensional stress field: the case of the Norcia seismic zone. *Annales Tectonicae* 8:38–57
- Buonasorte G, Fiordelisi A, Rossi U (1987) Tectonic structures and geometric setting of the Vulsini volcanic complex. *Periodico di Mineralogia* 56:123–136
- Buonasorte G, Cataldi R, Ceccarelli A, Costantini A, D'Offizi S, Lazzarotto A, Ridolfi A, Baldi P, Barelli A, Bertini G, Bertrami R, Calamai A, Cameli G, Coral R, D'Acquino C, Fiordelisi A, Ghezzi A, Lovari F (1988) Ricerca ed esplorazione nell'area geotermica di Torre Alfina (Lazio-Umbria), (in Italian). *Boll Soc Geol Ital* 107(2):265–237 (in Italian)
- Buonasorte G, Pandeli E, Fiordelisi A (1991) The Alfina 15 well: deep geological data from northern Latium (Torre Alfina geothermal area). *Boll Soc Geol Ital* 110:823–831
- Buonasorte G, Cameli GM, Ceron A, Cioni R, Pensieri R, Sbrana A (1995) Seismic reflection in the Bolsena Lake: a contribution to the knowledge of a caldera controlled geothermal system. *Proceedings of World Geothermal Congress, Florence* 2:833–842

- Cameli GM, Fiordelisi A (1988) Distribuzione delle anomalie geotermiche dell'alto Lazio, internal report. J.V. ENEL AGIP, Pisa (in Italian)
- Cameli GM, Dini I, Liotta D (1993) Upper crustal structure of the Larderello geothermal field as a feature of post-collisional extensional tectonics (southern Tuscany, Italy). *Tectonophysics* 224:413–423
- Carabelli E, Moia F, Fiordelisi A (1984) Seismic monitoring during geothermal wells stimulation as contribution to the individuation of prevailing fracturation trends. Presented at Seminar on Utilization of Geothermal Energy for Electric Power Production and Space Heating, Florence, Italy, May 14–17, pp 1–31
- Carapezza ML, Ranaldi M, Gattuso A, Pagliuca NM, Tarchini L (2015) The sealing capacity of the cap rock above the Torre Alfina geothermal reservoir (Central Italy) revealed by soil CO₂ flux investigations. *J Volcanol Geotherm Res* 291:25–34
- Carmignani L, Decandia FA, Disperati L, Fantozzi PL, Lazzarotto A, Liotta D, Meccheri M (1994) Tertiary extensional tectonics in Tuscany (Northern Apennines Italy). *Tectonophysics* 238:295–315
- Carmignani L, Conti P, Cornamusini G, Pirro A, (2013) Geological map of Tuscany (Italy). *Journal of Maps* 9(4): 487–497
- Chatelain J (1978) Étude fine de la sismicité en zone de collision continentale à l'aide d'un réseau de stations portables: la région Hindu-Kush-Pamir, Ph.D. thesis, Université Paul Sabatier, Toulouse (in French)
- Chiarabba C, Amato A, Fiordelisi A (1995) Upper crustal tomographic images of the Amiata-Vulsini geothermal region Central Italy. *J Geophys Res* 100(B3):4053–4066
- Chiarabba C, Jovane L, Di Stefano R (2005) A new view of Italian seismicity using 20 years of instrumental recordings. *Tectonophysics* 395:251–268
- Collettini C, Barchi M, Pauselli C, Federico C, Piali G (2000) Seismic expression of active extensional faults in northern Umbria (Central Italy). *J Geodyn* 29:309–321
- Console R, Murru M, Alessandrini B (1993) Foreshock statistics and their possible relationships to earthquake prediction in the Italian region. *Bull Seismol Soc Am* 83(4):1248–1263
- De Luca G, Scarpa R, Filippi L, Gorini A, Marcucci S, Marsan P, Milana G, Zambonelli E (1999) A detailed analysis of two seismic sequences in Abruzzo, Central Apennines, Italy. *Jose* 2:1–21
- Di Bucci D, Mazzoli S (2002) Active tectonics of the Northern Apennines and Adria geodynamics: new data and a discussion. *J Geodyn* 34:687–707
- Dialuce G, Chiarabba C, DiBucci D, Doglioni C, Gasparini P, Lanari R, Priolo E, Zollo A, (2014) Indirizzi e linee guida per il monitoraggio della sismicità, delle deformazioni del suolo e delle pressioni di poro nell'ambito delle attività antropiche. GdL MISE. Roma. URL: unmig.mise.gov.it/unmig/agenda/upload/85_238.pdf (in Italian)
- Faenza L, Pierdominici S (2007) Statistical occurrence analysis and spatio-temporal distribution of earthquakes in the Apennines (Italy). *Tectonophysics* 439:13–31
- Frepoli F, Amato A (1997) Contemporaneous extension and compression in the Northern Apennines from earthquake fault-plane solutions. *Geophys J Int* 139:483–498
- Galadini F, Galli P (2000) Active tectonics in the Central Apennines, Italy—input data for seismic hazard assessment. *Nat Hazards* 22:225–270
- Gasparini P (2002) Local magnitude reevaluation for recent Italian earthquakes (1981–1996). *J Seismol* 6:503–524
- Guidoboni E, Ferrari G, Mariotti D, Comastri A, Tarabusi G, Sgattoni G, Valensise G (2018) CFTI5Med, Catalogo dei Forti Terremoti in Italia (461 a.C.–1997) e nell'area Mediterranea (760 a.C.–1500). Istituto Nazionale di Geofisica e Vulcanologia (INGV) <http://storing.ingv.it/cfti/cfti5/>
- Hanks TC, Kanamori H (1979) A moment magnitude scale. *J Geophys Res* 84(B5):2348–2350
- ISIDe working group (2016). Italian seismological instrumental and parametric database, version 1.0, DOI: <https://doi.org/10.13127/ISIDe>. <http://cnt.rm.ingv.it/en/iside>
- Jolivet L, Faccenna C, Goffè B, Mattei M, Rossetti F, Brunet C, Storti F, Funicello R, Cadet JP, d'Agostino N, Parra T (1998) Midcrustal shear zones in post-orogenic extension: example from the northern Tyrrhenian Sea (Italy). *J Geophys Res* 103: 12123–12160
- Lahr JC (1999, revised 2012) HYPOELLIPSE: a computer program for determining local earthquake hypocentral parameters, magnitude, and first-motion pattern: U.S. Geological Survey Open-File Report 99–23, version 1.1, 119 p. and software, available at <https://pubs.usgs.gov/of/1999/of99-0023/>
- Lee WHK, Lahr JC (1975) HYP071 (Revised): a computer program for determining hypocenter, magnitude, and first motion pattern of local earthquakes. U. S. Geological Survey Open File Report 75–311, 113 pp
- Lee R, Bennett E, Meagher KL (1972) A method of estimating magnitude of local earthquakes from signal duration. Open File Report, U. S. Geological Survey, 28 pp
- Liotta D., 1994 Structural features of the Radicofani Basin along the Piancastagnaio (Mt.Amiata)-S. Casciano dei Bagni (Mt. Cetona) cross section. *Mem.Soc.Geol.It.*, 48/2, 401–408
- Liotta D (1996) Analisi del settore centro-meridionale del bacino pliocenico di Radicofani (Toscana meridionale). *Boll Soc Geol Ital* 115:115–143 (in Italian)
- Liotta D, Ranalli G (1999) Correlation between seismic reflectivity and rheology in extended lithosphere: southern Tuscany, inner northern Apennines, Italy. *Tectonophysics* 315:109–122
- Liotta D, Salvatorini G (1994) Evoluzione sedimentaria e tettonica della parte centro-meridionale del bacino pliocenico di Radicofani. *Studi Geologici Cemerti Vol Spec.* 1994(1):65–77 (in Italian)
- Malinverno A, Ryan WBF (1986) Extension in the Tyrrhenian Sea and shortening in the Apennines as result of arc migration driven by sinking of the lithosphere. *Tectonics* 5:227–254
- Martini IP, Saggi M (1993) Tectono-sedimentary characteristics of late Miocene-Quaternary extensional basins of the northern Apennines, Italy. *Earth Sci Rev* 34:197–233. [https://doi.org/10.1016/0012-8252\(93\)90034-5](https://doi.org/10.1016/0012-8252(93)90034-5)
- Nappi G, Renzulli A, Santi P (1991) Evidence of incremental growth in the Vulsinian calderas (Central Italy). Verma-Surendra, P, ed., calderas: genesis, structure and unrest. *J Volcanol Geotherm Res* 47:13–31
- Nappi G, Renzulli A, Santi P, Gillot PY (1995) Geological evolution and geochronology of the Vulsini Volcano District (Central Italy). *Boll Soc Geol Ital* 114:599–613

- Nicoletti M, Petrucciani C, Piro M, Trigila R (1981) Nuove datazioni vulsine per uno schema di evoluzione dell'attività vulcanica: Nota II: Il quadrante sud-occidentale: Periodico di Mineralogia. 50:141–169 (in Italian)
- Pace B, Peruzza L, Lavecchia G, Boncio P (2006) Layered seismogenic source model and probabilistic seismic-hazard analyses in Central Italy. *Bull Seismol Soc Am* 96:107–132
- Paige CC, Saunders MA (1982) LSQR: an algorithm for sparse linear equations and sparse least squares. *Trans Math Software* 8:43–71. <https://doi.org/10.1145/355984.355989>
- Palladino DM, Simei S (2005a) Eruptive dynamics and caldera collapse during the Onano eruption, Vulsini. *Italy Bull Volcanol* 67:423–440. <https://doi.org/10.1007/s00445-004-0385-3>
- Palladino DM, Simei S (2005b) The latera volcanic complex (Vulsini, Central Italy): eruptive activity and caldera evolution. *Acta Vulcanol* 17:75–80
- Pascucci V, Costantini A, Martini PI, Dringoli R (2006) Tectono-sedimentary analysis of complex, extensional, Neogene basin formed on thrust-faulted, Northern Apennines hinterland: Radicofani Basin, Italy. *Sediment Geol* 183:71–97
- Passerini P (1964) Il Monte Cetona (prov. di Siena). *Boll Soc Geol Ital* 83:219–338 (in Italian)
- Peccerillo A (2005) Plio-Quaternary volcanism in Italy: petrology, geochemistry, Geodynamics. Springer. doi <https://doi.org/10.1007/3-540-29092-3>
- Peccerillo A, Martinotti G (2006) The Western Mediterranean lamproitic magmatism: origin and geodynamic significance. *Terra Nova* 18:109–117
- Pontoise B, Monfret T (2004) Shallow seismogenic zone detected from an offshore-onshore temporary seismic network in the Esmeraldas area (northern Ecuador). *Geochem Geophys Geosyst* 5:Q02009. <https://doi.org/10.1029/2003GC000561>
- Raleigh CB, Healy JH, Bredehoeft JD (1976) An experiment in earthquake control at Rangely, Colorado. *Science* 191(4233): 1230–1237. <https://doi.org/10.1126/science.191.4233.1230>
- Reasenber PA, Oppenheimer D (1985) PPFIT, FPLOT and FPPAGE: Fortran computer programs for calculating and displaying earthquake fault-plane solutions. US Geological Survey Open-File Report 85–739: 25 pp
- Rovida A, Locati M, Camussi R, Lolli B, Gasperini P (eds) (2016) CPTI15, the 2015 version of the parametric catalogue of Italian earthquakes. Istituto Nazionale di Geofisica e Vulcanologia doi <https://doi.org/10.6092/INGV.IT-CPTI15>
- Selvaggi G, Amato A (1992) Subcrustal earthquakes in the northern Apennines (Italy): evidence for a still active subduction? *Geophys Res Lett* 19:2127–2130
- Sparks RSJ (1975) Stratigraphy and geology of the ignimbrites of Vulsini volcano, Central Italy. *Geol Rundsch* 64:497–523
- Terlizze F (2016) Linee guida per l'utilizzazione della risorsa geotermica a media e alta entalpia, GdL Mise, Roma. <http://unmig.mise.gov.it/unmig/geotermia/lineeguida.pdf> (in Italian)
- Toro B (1978) Residual gravity anomalies and deep structure in the volcanic region of northern Latium. *Geol Romana* 17:35–44
- Trigila R (1985) Vulsini volcanoes, in 1995 International Association of Volcanology and Chemistry of the Earth's interior scientific assembly, Giardini-Naxos (Italy), Excursion Guidebook, 4–12
- Varekamp JC (1980) The geology of the Vulsinian area, Lazio, Italy. *Bull Volcanol* 43(3):489–503. <https://doi.org/10.1007/BF02597687>
- Vignaroli G, Pinton A, De Benedetti AA, Giordano G, Rossetti F, Soligo M, Berardi G (2013) Structural compartmentalisation of a geothermal system, the Torre Alfina field (Central Italy). *Tectonophysics* 608:482–498
- Vignaroli G, Berardi G, Billi A, Kele S, Rossetti F, Soligo M, Bernasconi SM, (2016) Tectonics, hydrothermalism, and paleoclimate recorded by Quaternary travertines and their spatio-temporal distribution in the Albegna basin, central Italy: Insights on Tyrrhenian margin neotectonics. *Lithosphere* 8(4):335–358
- Volpi G, Magri F, Colucci F, Fisher T, de Caro M, Crosta GB (2018) Modeling highly buoyant flows in the Castel Giorgio: Torre Alfina deep geothermal reservoir. *Geofluids* 2018: 3818629, 19 pages. <https://doi.org/10.1155/2018/3818629>
- Waldhauser F (2001) HypoDD: a program to compute double-difference hypocenter locations. U.S. Geol. Surv, Open File Rep. 01–113, Menlo Park, California
- Waldhauser F, Ellsworth WL (2000) A double-difference earthquake location algorithm: method and application to the northern Hayward fault, California. *Bull Seismol Soc Am* 90:1353–1368. <https://doi.org/10.1785/0120000006>
- Washington HS (1906) The Roman comagmatic region: Carnegie Institution of Washington publication 57:199 pp

Publisher's note Springer Nature remains neutral with regard to jurisdictional claims in published maps and institutional affiliations.